

Ground state of two electrons on a sphere

Pierre-François Loos and Peter M. W. Gill*

Research School of Chemistry, Australian National University, Canberra ACT 0200, Australia

(Dated: March 25, 2022)

We have performed a comprehensive study of the singlet ground state of two electrons on the surface of a sphere of radius R . We have used electronic structure models ranging from restricted and unrestricted Hartree-Fock theory to explicitly correlated treatments, the last of which lead to near-exact wavefunctions and energies for any value of R . Møller-Plesset energy corrections (up to fifth-order) are also considered, as well as the asymptotic solution in the large- R regime.

PACS numbers: 31.15.ac, 31.15.ve, 31.15.xp, 31.15.xr, 31.15.xt

Keywords: electron correlation, cusp condition, Hartree-Fock solution, symmetry-broken solution, perturbation theory, Møller-Plesset, asymptotic expansion, configuration interaction, explicitly correlated methods, Hylleraas expansion.

I. INTRODUCTION

Exactly (or very accurately) solvable models have ongoing value and are valuable both for illuminating more complicated systems and for testing theoretical approaches, such as density functional methods [1–3]. One such model is the Hooke’s law atom (or Harmonium) which is composed of two electrons bound to a nucleus by a harmonic potential but repelling Coulombically. This system was first considered more than 40 years ago by Kestner and Sinanoglu [4], but solved analytically in 1989 by Kais *et al.* [5] for a particular value of the harmonic force constant and, later, for a countably infinite set force constants [6].

A related system, studied by Alavi and co-workers [7–9], consists of two electrons, interacting through a Coulomb potential, but confined within a ball of radius R . This possesses a number of interesting features, including the formation of a “Wigner molecule” for large R [10]. The spontaneous formation of such molecules can also occur in quantum dots and is analogous to the Wigner crystallization [11] of the uniform electron gas.

If the two electrons are constrained to remain on the *surface* of the sphere, one obtains a model that Berry and co-workers have used [12–15] to understand both weakly and strongly correlated systems, such as the ground and excited states of the helium atom, and also to suggest the “alternating” version of Hund’s rule [16]. Seidl studied this system in the context of density functional theory [17] in order to test the ISI (interaction-strength interpolation) model [18]. For this purpose, he derived accurate solutions in both the weak interaction limit (the small R regime) and the strong interaction limit (the large R regime). He also obtained accurate results by numerical integration of the Schrödinger equation.

In this paper, we are interested in the 1S ground state of two electrons on the surface of a sphere of radius R . This allows us to restrict our study to the symmetric

spatial part of the wavefunction and ignore the spin coordinates. We have extended Seidl’s analysis and performed an exhaustive study using a range of models. We restrict our analysis to the repulsive potential case; the strong-attraction limit (attractive potential) is carefully examined in Ref. [17].

Restricted and unrestricted Hartree-Fock (HF) solutions are discussed in Section III and the strengths and weaknesses of Møller-Plesset (MP) perturbation theory [19] in Section IV. We consider asymptotic solutions for large R in Section V and, in Section VI, we explore several variational schemes including explicitly correlated techniques [20–24]) that enforce the cusp condition [25, 26]. Atomic units are used throughout.

II. HAMILTONIAN

The absolute position of the i -th electron is defined by its spherical polar angles $\Omega_i = (\theta_i, \phi_i)$. The relative position of the electrons is conveniently measured by the interelectronic angle θ which they subtend at the origin. These coordinates are related by

$$\cos \theta = \cos \theta_1 \cos \theta_2 + \sin \theta_1 \sin \theta_2 \cos(\phi_1 - \phi_2) \quad (1)$$

and we have $0 \leq u \equiv |\mathbf{r}_1 - \mathbf{r}_2| \leq 2R$.

The Hamiltonian is

$$\hat{H} = \hat{T} + u^{-1} \quad (2)$$

where

$$\hat{T} = \hat{T}_1 + \hat{T}_2 = -\frac{\nabla_1^2}{2} - \frac{\nabla_2^2}{2} \quad (3)$$

is the kinetic operator for both electrons and u^{-1} is the Coulomb operator. In terms of θ , the Hamiltonian is

$$\hat{H} = -\frac{1}{R^2} \left(\frac{d^2}{d\theta^2} + \cot \theta \frac{d}{d\theta} \right) + \frac{1}{2R} \csc \frac{\theta}{2} \quad (4)$$

in which form it becomes clear that the kinetic and potential parts of \hat{H} scale with R^{-2} and R^{-1} , respectively.

*Corresponding author; Electronic address: peter.gill@anu.edu.au

III. HARTREE-FOCK APPROXIMATIONS

A. Restricted Hartree-Fock

In the HF approximation, each electron feels the mean field generated by the other electron [27]. The restricted Hartree-Fock (RHF) solution

$$\Phi^{\text{RHF}}(\Omega_1, \Omega_2) = \Psi^{\text{RHF}}(\Omega_1) \Psi^{\text{RHF}}(\Omega_2) \quad (5)$$

places both electrons in an orbital Ψ^{RHF} that is an eigenfunction of the Fock operator

$$\hat{F}_1 = \hat{T}_1 + \int \frac{|\Psi^{\text{RHF}}(\Omega_2)|^2}{u} R^2 d\Omega_2 \quad (6)$$

with $d\Omega_2 = \sin \theta_2 d\theta_2 d\phi_2$.

By definition, the one-electron basis function

$$\Psi_{\ell m}(\Omega_i) = \frac{Y_{\ell m}(\Omega_i)}{R} \quad (7)$$

where $Y_{\ell m}$ is the spherical harmonic of degree ℓ and order m is an eigenfunction of \hat{T}_i with eigenvalue $\ell(\ell+1)/(2R^2)$. Using the partial-wave expansion [28]

$$u^{-1} = R^{-1} \sum_{\ell=0}^{\infty} P_{\ell}(\cos \theta) \quad (8)$$

and the addition theorem [29]

$$P_{\ell}(\cos \theta) = \frac{4\pi}{2\ell+1} \sum_{m=-\ell}^{+\ell} Y_{\ell m}^*(\Omega_1) Y_{\ell m}(\Omega_2) \quad (9)$$

it is straightforward to show that

$$\int \frac{|\Psi_{00}(\Omega_2)|^2}{u} R^2 d\Omega_2 = \frac{1}{R} \quad (10)$$

The orbital $\Psi_{00}(\Omega_i)$ is thus an eigenfunction of \hat{F}_i with the eigenvalue $1/R$. Moreover, it follows from the orthogonality of the spherical harmonics that

$$\left\langle \Psi_{\ell m}(\Omega_1) \left| \hat{F}_1 \right| \Psi_{00}(\Omega_1) \right\rangle = \delta_{\ell,0} \delta_{m,0} \quad (11)$$

which ensures the stationarity of the RHF energy with respect to the orbitals $\Psi_{\ell m}$.

The ground-state RHF energy is thus

$$E^{\text{RHF}} = \frac{1}{R} \quad (12)$$

and the normalized RHF wavefunction is

$$\Phi^{\text{RHF}} = \frac{1}{4\pi R^2} \quad (13)$$

which yields a uniform electron density over the surface of the sphere.

B. Unrestricted Hartree-Fock

When R exceeds a critical value, a second, unrestricted HF (UHF) solution develops [30–32] in which the two electrons tend to localize on opposite sides of the sphere. This is analogous to the UHF description of a dissociating H_2 molecule [27].

To obtain this symmetry-broken solution

$$\Phi^{\text{UHF}}(\theta_1, \theta_2) = \Psi^{\text{UHF}}(\theta_1) \Psi^{\text{UHF}}(\pi - \theta_2) \quad (14)$$

we expand the orbital as

$$\Psi^{\text{UHF}}(\theta_i) = \sum_{\ell=0}^{\infty} C_{\ell} \Psi_{\ell}(\theta_i) \quad (15)$$

where the $\Psi_{\ell}(\theta_i) = Y_{\ell}(\theta_i)/R = Y_{\ell 0}(\Omega_i)/R$ are zonal spherical harmonics. The Fock matrix elements in this basis are

$$\begin{aligned} F_{\ell_1 \ell_2} &= \left\langle \Psi_{\ell_1}(\theta_1) \left| \hat{F}_1 \right| \Psi_{\ell_2}(\theta_1) \right\rangle \\ &= \frac{\ell_1(\ell_1+1)}{2R^2} \delta_{\ell_1, \ell_2} + \sum_{\ell_3, \ell_4=0}^{\infty} C_{\ell_3} C_{\ell_4} G_{\ell_1 \ell_2}^{\ell_3 \ell_4} \end{aligned} \quad (16)$$

where the two-electron integrals are

$$G_{\ell_1 \ell_2}^{\ell_3 \ell_4} = \left\langle \Psi_{\ell_1}(\theta_1) \Psi_{\ell_3}(\theta_2) \left| u^{-1} \right| \Psi_{\ell_2}(\theta_1) \Psi_{\ell_4}(\theta_2) \right\rangle \quad (17)$$

Using the partial-wave expansion (8) and the relation

$$\begin{aligned} \langle \ell_1 \ell_2 \ell_3 \rangle &= \int Y_{\ell_1}(\theta) Y_{\ell_2}(\theta) Y_{\ell_3}(\theta) \sin \theta d\theta \\ &= \sqrt{\frac{(2\ell_1+1)(2\ell_2+1)(2\ell_3+1)}{4\pi}} \begin{pmatrix} \ell_1 & \ell_2 & \ell_3 \\ 0 & 0 & 0 \end{pmatrix}^2 \end{aligned} \quad (18)$$

between the integrals of three spherical harmonics and the Wigner 3j-symbols [33], we find

$$G_{\ell_1 \ell_2}^{\ell_3 \ell_4} = \frac{(-1)^{\ell_3+\ell_4}}{R} \sum_{\ell=0}^{\infty} \frac{4\pi}{2\ell+1} \langle \ell_1 \ell_2 \ell \rangle \langle \ell_3 \ell_4 \ell \rangle \quad (19)$$

where selection rules [33] restrict the terms in the sum.

The UHF energy is then given by

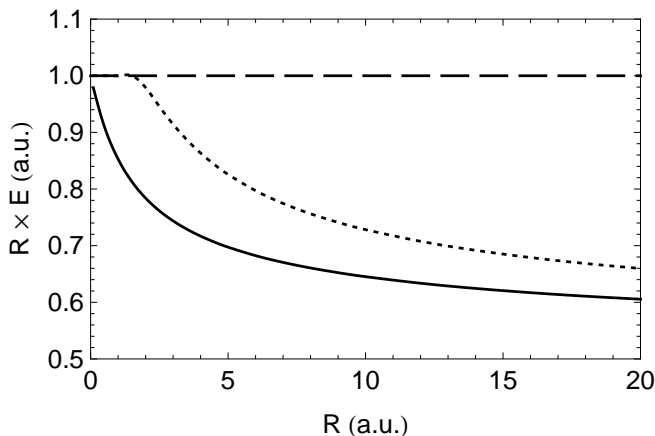
$$E^{\text{UHF}} = \sum_{\ell=0}^{\infty} C_{\ell}^2 \frac{\ell(\ell+1)}{R^2} + \sum_{\ell_1, \ell_2=0}^{\infty} C_{\ell_1} C_{\ell_2} F_{\ell_1 \ell_2} \quad (20)$$

The first term is the kinetic energy and is positive. However, for sufficiently large R , this is outweighed by negative contributions in the second term and it is these that drive the symmetry-breaking process.

For computational reasons, we truncate the sum in (15) at $\ell = L$ but, for all of the radii R considered in this study, we found that $L = 15$ suffices to obtain E^{UHF} with an accuracy of 10^{-12} .

TABLE I: RHF, UHF and exact energies for various R .

R	E^{RHF}	E^{UHF}	E^{exact}
0.0001	10000	10000	9999.772 600 495
0.001	1000	1000	999.772 706 409
0.01	100	100	99.773 761 078
0.1	10	10	9.783 873 673
0.2	5	5	4.794 237 154
0.5	2	2	1.820 600 768
1	1	1	0.852 781 065
2	0.500 000	0.489 551	0.391 958 796
3	0.333 333	0.304 783	0.247 897 526
4	0.250 000	0.215 864	0.179 210 308
5	0.200 000	0.165 161	0.139 470 826
10	0.100 000	0.072 829	0.064 525 123
20	0.050 000	0.032 983	0.030 271 992
50	0.020 000	0.012 006	0.011 363 694
100	0.010 000	0.005 708 105	0.005 487 412
1000	0.001 000	0.000 522 363	0.000 515 686

FIG. 1: $R \times E^{\text{RHF}}$ (dashed), $R \times E^{\text{UHF}}$ (dotted) and $R \times E^{\text{exact}}$ (solid) as a function of R .

As Table I and Figure 1 show, the UHF solution becomes lower than the RHF one for $R > R^{\text{crit}} \approx 1.5$ and the UHF, not RHF, energy behaves correctly for large R . Specifically, it can be shown that

$$\lim_{R \rightarrow \infty} R E^{\text{RHF}} = 1 \quad (21)$$

$$\lim_{R \rightarrow \infty} R E^{\text{UHF}} = 1/2 \quad (22)$$

The UHF result reflects the Coulomb interaction between two electrons localized on opposite sides of the sphere [17], a phenomenon known as Wigner crystallization [10, 11]. The difference between the UHF and exact energies (*i.e.* the correlation energy) appears to decay as $O(R^{-3/2})$.

IV. EXPANSION FOR SMALL R

In Møller-Plesset perturbation theory, the Hamiltonian of the system is partitioned as

$$\hat{H} = \hat{H}_0 + \hat{V} \quad (23)$$

where \hat{H}_0 the zeroth-order Hamiltonian and \hat{V} is a perturbation operator and, in our case, we have

$$\hat{H}_0 = \hat{T} \quad (24)$$

$$\hat{V} = u^{-1} \quad (25)$$

The ground-state wavefunction and energy are expanded

$$\Phi = \Phi^{(0)} + \Phi^{(1)} + \Phi^{(2)} + \Phi^{(3)} + \dots \quad (26)$$

$$E = E^{(0)} + E^{(1)} + E^{(2)} + E^{(3)} + \dots \quad (27)$$

We will refer to $E^{(n)}$ as the n th-order energy and define the MP n correlation energy as

$$E^{\text{MP}n} = \sum_{m=2}^n E^{(m)} \quad (28)$$

Dimensional analysis reveals that

$$\Phi = \frac{\phi_0}{R^2} + \frac{\phi_1}{R} + \phi_2 + \phi_3 R + \phi_4 R^2 + \phi_5 R^3 + \dots \quad (29)$$

$$E = \frac{\varepsilon_0}{R^2} + \frac{\varepsilon_1}{R} + \varepsilon_2 + \varepsilon_3 R + \varepsilon_4 R^2 + \varepsilon_5 R^3 + \dots \quad (30)$$

where the ϕ_n are functions of θ and the ε_n are numbers. From (12) and (13), we see $\phi_0 = 1/4\pi$, $\varepsilon_0 = 0$ and $\varepsilon_1 = 1$.

The excited eigenfunctions of \hat{H}_0 are given by

$$\Phi_{\ell_1 m_1}^{\ell_2 m_2}(\Omega_1, \Omega_2) = \Psi_{\ell_1 m_1}(\Omega_1) \Psi_{\ell_2 m_2}(\Omega_2) \quad (31)$$

and we can expand the exact wavefunction Φ in this basis. However, for the 1S ground state, angular momentum theory [33, 34] limits the combinations of ℓ_1 , ℓ_2 , m_1 and m_2 that contribute and it is more efficient to expand Φ in the basis of two-electron functions

$$\Phi_\ell(\theta) = \frac{\sqrt{2\ell+1}}{4\pi R^2} P_\ell(\cos \theta) \quad (32)$$

which are eigenfunctions of \hat{T} with eigenvalues

$$E_\ell = \frac{\ell(\ell+1)}{R^2} \quad (33)$$

A. First-order wavefunction

In the intermediate normalization, the first-order wavefunction is

$$\begin{aligned} \Phi^{(1)}(\theta) &\equiv \frac{\phi_1(\theta)}{R} = \sum_{\ell=1}^{\infty} \frac{\langle \Phi^{\text{RHF}} | \hat{V} | \Phi_\ell \rangle}{E_0 - E_\ell} \Phi_\ell(\theta) \\ &= -\frac{1}{4\pi R} \sum_{\ell=1}^{\infty} \frac{1}{\ell(\ell+1)} P_\ell(\cos \theta) \end{aligned} \quad (34)$$

Using the Legendre generating function

$$\sum_{\ell=0}^{\infty} P_{\ell}(x) t^{\ell} = \frac{1}{\sqrt{1-2xt+t^2}} \quad (35)$$

the sum in (34) can be found in closed-form, yielding

$$\Phi^{(1)}(\theta) = \frac{1}{4\pi R} \left[2 \ln \left(1 + \sin \frac{\theta}{2} \right) - 1 \right] \quad (36)$$

or, equivalently,

$$\Phi^{(1)}(u) = \frac{1}{4\pi R} \left[2 \ln \left(1 + \frac{u}{2R} \right) - 1 \right] \quad (37)$$

and these yield the normalized first-order wavefunction

$$\Phi^{\text{MP1}}(\theta) = \frac{\Phi^{\text{RHF}} + \Phi^{(1)}(\theta)}{\sqrt{1 + (16 \ln 2 - 11)R^2}} \quad (38)$$

The true ground-state wavefunction must be nodeless. However, it is easy to show that the MP1 wavefunction possesses a node if $R > 1$, leading us to anticipate that Φ^{MP1} will be a poor wavefunction for large spheres.

B. Second- and third-order energies

According to the Wigner $2n+1$ rule [35], the 1st-order wavefunction generates the 2nd- and 3rd-order energies. The 2nd-order energy, which has previously been found by Seidl [17], is given by

$$\begin{aligned} E^{(2)} \equiv \varepsilon_2 &= \left\langle \Phi^{\text{RHF}} \left| \hat{V} \right| \Phi^{(1)} \right\rangle \\ &= 4\mathcal{L} - 3 \\ &= -0.227\,411\,278\dots \end{aligned} \quad (39)$$

where $\mathcal{L} = \ln 2$. As Table II shows, the MP2 correlation energy is an excellent approximation for small R but, because it is independent of R , it is poor for large R .

It is surprising to find that $E^{(2)}$ is so much larger than the limiting correlation energies [36] of the helium-like ions (-0.0467) or Hooke's Law atoms (-0.0497).

The 3rd-order energy is given by

$$E^{(3)} \equiv \varepsilon_3 R = \left\langle \Phi^{(1)} \left| \hat{V} - E^{(1)} \right| \Phi^{(1)} \right\rangle \quad (40)$$

and this yields

$$\begin{aligned} \varepsilon_3 &= 8(\mathcal{L}^2 - 5\mathcal{L} + 3) \\ &= +0.117\,736\,889\dots \end{aligned} \quad (41)$$

which agrees with Seidl's rough estimate [17]. Table II shows that MP3 gives an improvement over MP2 but that it, too, eventually breaks down as R increases.

C. Second-order wavefunction

To find the 4th- and 5th-order energies, we need the 2nd-order wavefunction. This is given by

$$\Phi^{(2)}(\theta) = \sum_{\ell=1}^{\infty} \frac{\left\langle \Phi^{(1)} \left| \hat{V} - E^{(1)} \right| \Phi_{\ell} \right\rangle}{E_0 - E_{\ell}} \Phi_{\ell}(\theta) \quad (42)$$

which yields

$$\begin{aligned} \Phi^{(2)}(\theta) &= \frac{1}{4\pi} \sum_{\ell_1, \ell_2=1}^{\infty} \sum_{\ell=|\ell_1-\ell_2}^{\ell_1+\ell_2} \\ &\quad \times \frac{2\ell_2+1}{\ell_1(\ell_1+1)\ell_2(\ell_2+1)} \begin{pmatrix} \ell_1 & \ell_2 & \ell \\ 0 & 0 & 0 \end{pmatrix}^2 P_{\ell_2}(\cos \theta) \end{aligned} \quad (43)$$

Using the identity

$$\sum_{\ell=1}^{\infty} \frac{2\ell+1}{\ell(\ell+1)} P_{\ell}(x)P_{\ell}(y) = -\ln \frac{(1-x)(1+y)}{4} - 1 \quad (44)$$

for $x \leq y$, we eventually obtain

$$\begin{aligned} \Phi^{(2)}(u) &= (2\mathcal{L}^2 - 2\mathcal{L} + 5)\phi_0 + (2\mathcal{L} - 5)\phi_1(u) - \frac{\pi}{4} \\ &\quad + \frac{1}{\pi} \left[\text{Li}_2 \left(\frac{1}{2} - \frac{u}{4R} \right) - 2 \text{Li}_2 \left(-\frac{u}{2R} \right) \right] \end{aligned} \quad (45)$$

where Li_2 is the dilogarithm function [37].

D. Fourth- and fifth-order energies

The Wigner $2n+1$ rule and the closed-form expression of $\Phi^{(2)}$ yield the 4th- and 5th-order coefficients

$$\begin{aligned} \varepsilon_4 &= \frac{16}{3}(4\mathcal{L}^3 - 42\mathcal{L}^2 + 96\mathcal{L} - 45) - 12\zeta(3) \\ &= -0.050\,275\,600\dots \end{aligned} \quad (46)$$

$$\begin{aligned} \varepsilon_5 &= \frac{32}{3}(5\mathcal{L}^4 - 90\mathcal{L}^3 + 450\mathcal{L}^2 - 660\mathcal{L} + 252) \\ &\quad + (216 - 80\mathcal{L})\zeta(3) \\ &= +0.013\,957\,832\dots \end{aligned} \quad (47)$$

where ζ is the Riemann zeta function.

The MP_n correlation energies for various values of R are reported in Table II and illustrated in Figure 2. The results show that MP4 and MP5 are very accurate for small R and, indeed, the latter is reasonable up to $R \approx 1$.

The MP expansion converges for radii R within the radius of convergence

$$R^{\text{cvg}} = \lim_{n \rightarrow \infty} \left| \frac{\varepsilon_n}{\varepsilon_{n+1}} \right| \quad (48)$$

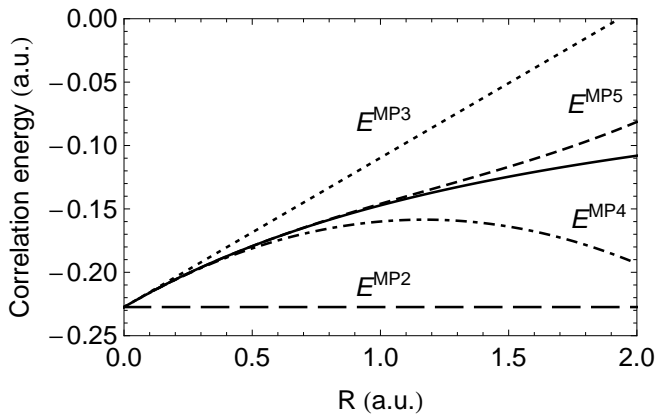
From our results, it seems that $R^{\text{cvg}} > 2$, but it is not possible to be more precise than this [17, 18].

TABLE II: Correlation energies (relative to UHF and multiplied by -1) from various models for various R .

R	MP2	MP3	MP4	MP5	Hylleraas	Seidl	Exact ^a
0.0001	0.227 411	0.227 399 504 071	0.227 399 504 574	0.227 399 504 574	0.222 212	—	0.227 399 504 574
0.001	0.227 411	0.227 293 541	0.227 293 591 147	0.227 293 591 133	0.222 123	—	0.227 293 591 133
0.01	0.227 411	0.226 234	0.226 238 936	0.226 238 922 473	0.221 237	—	0.226 238 922 463
0.1	0.227 411	0.215 638	0.216 140	0.216 126 387	0.212 574	0.2175 ^b	0.216 126 326 630
0.2	0.227 411	0.203 864	0.205 875	0.205 763 261	0.203 406	0.2064 ^b	0.205 762 846 030
0.5	0.227 411	0.168 543	0.181 112	0.179 367	0.178 908	0.1796 ^b	0.179 399 232 168
1	0.227 411	0.109 674	0.159 950	0.145 992	0.147 181	0.1473 ^b	0.147 218 934 944
	$e - e$	LR0	LR1	LR2			
2	0.239 551	0.062 774	0.094 024	0.095 405	0.096 444	0.0977 ^c	0.097 591 955 594
3	0.138 116	0.041 890	0.055 780	0.056 281	0.054 783	—	0.056 885 070 442
4	0.090 864	0.028 352	0.036 176	0.036 420	0.033 984	—	0.036 653 426 934
5	0.065 161	0.020 440	0.025 440	0.025 580	0.022 707	0.0257 ^c	0.025 690 364 031
10	0.022 829	0.007 018	0.008 268	0.008 292	0.005 129	0.0083 ^c	0.008 303 955 973
20	0.007 983	0.002 393	0.002 706	0.002 710	0.000 154	—	0.002 711 198 384
50	0.002 006	0.000 592	0.000 642 054	0.000 642 496	-0.000 860	—	0.000 642 573 605
100	0.000 708	0.000 187	0.000 220 605	0.000 220 683	-0.000 679	—	0.000 220 692 615
1000	0.000 022	0.000 006 552	0.000 006 677 055	0.000 006 677 302	-0.000 112	—	0.000 006 677 311

^aFrom the polynomial wavefunction in Section VID^bNative result of Ref. [17].^cCorrelation energy form Ref. [17] relative to the UHF energy.

FIG. 2: MP_n correlation energies as a function of R . The exact correlation energy is shown as the solid curve.



V. EXPANSION FOR LARGE R

A. Harmonic approximation

For large R (LR), the potential dominates the kinetic energy and the electrons tend to localize on opposite sides of the sphere. The classical mechanical energy would be

$$E^{e-e} = \frac{1}{2R} \quad (49)$$

but, quantum mechanically, the kinetic energies of the electrons cannot vanish and each electron therefore maintains a zero-point oscillation around its equilibrium position with an angular frequency ω . Such phenomena are ubiquitous in strongly correlated systems, as demonstrated by Seidl and his co-workers [17, 18, 38–40].

In this limit, the supplementary angle $\xi = \pi - \theta$ is the natural coordinate and the Hamiltonian becomes

$$\hat{H} = -\frac{1}{R^2} \left(\frac{d^2}{d\xi^2} + \cot \xi \frac{d}{d\xi} \right) + \frac{1}{2R} \sec \frac{\xi}{2} \quad (50)$$

For small oscillations ($\xi \simeq 0$), the Taylor series

$$\cot \xi = \xi^{-1} - \xi/3 - \xi^3/45 + \dots \quad (51)$$

$$\sec(\xi/2) = 1 + \xi^2/8 + 5\xi^4/384 + 61\xi^6/46080 + \dots \quad (52)$$

yield the harmonic-oscillator Hamiltonian

$$\hat{H}^\omega = -\frac{1}{R^2} \left(\frac{d^2}{d\xi^2} + \frac{1}{\xi} \frac{d}{d\xi} \right) + \frac{1}{2R} \left(1 + \frac{\xi^2}{8} \right) \quad (53)$$

whose ground-state wavefunction and energy are

$$\Phi_0^\omega(\xi) = \frac{1}{2\sqrt{2\pi}R^{7/4}} \exp(-\sqrt{R}\xi^2/8) \quad (54)$$

$$E^{\text{LR}0} \equiv \mathcal{E}^{(0)} = \frac{1}{2R} + \frac{1}{2R^{3/2}} \quad (55)$$

The second term is the zero-point energy associated with harmonic oscillations of angular frequency $\omega = 1/R^{3/2}$ and it appears that this is the leading error in the UHF description at large R .

B. First and second anharmonic corrections

By analogy with the small- R expansion (30), we would like to construct a large- R asymptotic expansion

$$\begin{aligned} E &\sim \mathcal{E}^{(0)} + \mathcal{E}^{(1)} + \mathcal{E}^{(2)} + \dots \\ &= \frac{\eta_1}{R} + \frac{\eta_2}{R^{3/2}} + \frac{\eta_3}{R^2} + \frac{\eta_4}{R^{5/2}} + \dots \end{aligned} \quad (56)$$

where we know $\eta_1 = \eta_2 = 1/2$. The n th excited state of the Hamiltonian (53) has the wavefunction and energy

$$\Phi_n^\omega(\xi) = L_n(\sqrt{R}\xi^2/4) \Phi_0^\omega(\xi) \quad (57)$$

$$E_n^\omega = \left(n + \frac{1}{2} \right) \omega \quad (58)$$

where L_n is the Laguerre polynomial of degree n [29]. The anharmonic corrections, $\mathcal{E}^{(1)}$ and $\mathcal{E}^{(2)}$, can be found [41] using the perturbation operators

$$\hat{W}^{(1)} = -\frac{1}{R^2} \frac{\xi}{3} \frac{d}{d\xi} + \frac{1}{2R} \frac{5\xi^4}{384} \quad (59)$$

$$\hat{W}^{(2)} = -\frac{1}{R^2} \frac{\xi^3}{45} \frac{d}{d\xi} + \frac{1}{2R} \frac{61\xi^6}{46080} \quad (60)$$

The first-order correction is

$$\begin{aligned} \mathcal{E}^{(1)} &= \left\langle \Phi_0^\omega \left| \hat{W}^{(1)} \right| \Phi_0^\omega \right\rangle \\ &= 4\pi^2 R^4 \int_0^\infty \Phi_0^\omega(\xi) \hat{W}^{(1)} \Phi_0^\omega(\xi) \xi d\xi \end{aligned} \quad (61)$$

and this yields $\eta_3 = -1/8$ and therefore

$$E^{\text{LR}1} = \frac{1}{2R} + \frac{1}{2R^{3/2}} - \frac{1}{8R^2} \quad (62)$$

The second-order correction is

$$\mathcal{E}^{(2)} = \sum_{n=1}^{\infty} \frac{\left\langle \Phi_0^\omega \left| \hat{W}^{(1)} \right| \Phi_n^\omega \right\rangle^2}{E_0^\omega - E_n^\omega} + \left\langle \Phi_0^\omega \left| \hat{W}^{(2)} \right| \Phi_0^\omega \right\rangle \quad (63)$$

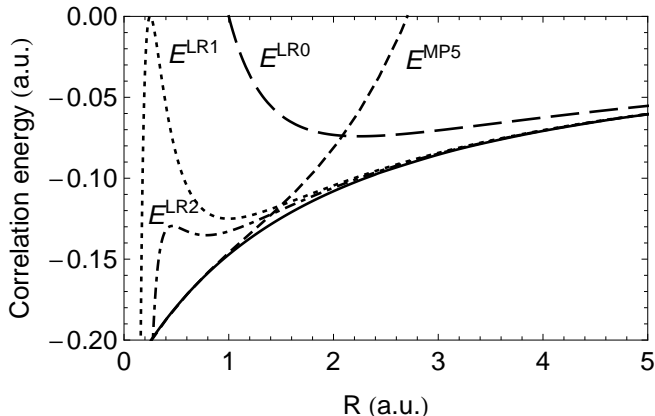
but because of the orthogonality and recurrence relations of Laguerre polynomials [29], only the first two terms in the sum in (63) are non-zero and one finds $\eta_4 = -1/128$ and therefore

$$E^{\text{LR}2} = \frac{1}{2R} + \frac{1}{2R^{3/2}} - \frac{1}{8R^2} - \frac{1}{128R^{5/2}} \quad (64)$$

From the results in Table II and Figure 3, it seems that the asymptotic expansion converges toward the exact energy and is reasonably accurate for $R > 3$.

Through judicious use of the 5th-order truncation of (30) and the 2nd-order truncation of (56), one can predict satisfactory energies over a wide range of R values. However, there remains a region ($1 \lesssim R \lesssim 3$) where both the small- R and large- R solutions are inadequate.

FIG. 3: Correlation energies (relative to RHF) from E^{LR0} (dashed), E^{LR1} (dotted) and E^{LR2} (dot-dashed), E^{MP5} (small dash) and E^{exact} (solid) as a function of R .



VI. VARIATIONAL WAVEFUNCTIONS

A. Configuration interaction

We begin with a configuration interaction (CI) treatment wherein the wavefunction is expanded as

$$\Phi_L^{\text{CI}}(\theta) = \sum_{\ell=0}^L T_\ell \Phi_\ell(\theta) \quad (65)$$

in the Legendre polynomial basis set (32). The resulting energy E_L^{CI} is the lowest eigenvalue of the CI matrix

$$\begin{aligned} \langle \Phi_{\ell_1} | \hat{H} | \Phi_{\ell_2} \rangle &= \frac{\ell_1(\ell_1+1)}{R^2} \delta_{\ell_1, \ell_2} \\ &+ \frac{1}{R} \sum_{\ell=|\ell_1-\ell_2|}^{\ell_1+\ell_2} \sqrt{\frac{4\pi}{2\ell+1}} \langle \ell_1 \ell_2 \ell \rangle \end{aligned} \quad (66)$$

where $\langle \ell_1 \ell_2 \ell \rangle$ is defined by (18).

The CI energy as the maximum angular momentum L increases is reported in Table III. It converges very slowly and even $L = 40$ yields an accuracy of only 10^{-4} . The reason for this slow convergence – the failure of (65) to satisfy the Kato cusp condition – is well known.

B. Hylleraas

The simplest possible wavefunction with a cusp is

$$\Phi^{\text{Hy}} = 1 + \gamma u \quad (67)$$

which has an explicit linear dependence on the interelectronic distance u . Kato proved [25] that $\gamma = 1/2$ in normal singlet states but, because our electrons are confined to a sphere, this γ does not apply (see below).

Using the partial-wave expansion

$$u = R \sum_{\ell=0}^{\infty} \left(\frac{1}{2\ell+3} - \frac{1}{2\ell-1} \right) P_\ell(\cos \theta) \quad (68)$$

TABLE III: Convergence of correlation energies with respect to the number L of terms in the CI, R12-CI and Hylleraas wavefunctions. All results pertain to the sphere with $R = 1$.

L	CI	R12-CI	Polynomial
0	-0.000 000	-0.147 180 860	-0.000 000 000 000
1	-0.131 665	-0.147 185 454	-0.147 180 859 845
2	-0.141 241	-0.147 202 916	-0.147 218 627 134
3	-0.144 065	-0.147 209 904	-0.147 218 930 072
4	-0.145 273	-0.147 213 200	-0.147 218 934 845
5	-0.145 900	-0.147 214 987	-0.147 218 935 941
10	-0.146 847	-0.147 217 796	-0.147 218 935 944
15	-0.147 047	-0.147 218 405	-0.147 218 935 944
20	-0.147 120	-0.147 218 631	-0.147 218 935 944
25	-0.147 155	-0.147 218 738	-0.147 218 935 944
30	-0.147 174	-0.147 218 797	-0.147 218 935 944
35	-0.147 186	-0.147 218 833	-0.147 218 935 944
40	-0.147 194	-0.147 218 857	-0.147 218 935 944

one finds that the energy is

$$E^{\text{Hy}}(\gamma) = \frac{6 + 3\gamma(\gamma+4)R + 8\gamma^2 R^2}{2R(3 + 8\gamma R + 6\gamma^2 R^2)} \quad (69)$$

and minimizing this with respect to γ yields

$$\gamma^{\text{opt}} = \frac{12}{9 - 12R + \sqrt{81 + 72R + 48R^2}} \quad (70)$$

$$E^{\text{Hy}} = \frac{9 + 12R - \sqrt{81 + 72R + 48R^2}}{8R^2} \quad (71)$$

Correlation energies obtained from (71) for several values of R are reported in Table II. Despite the simplicity of the wavefunction, its energies are surprisingly good with a maximum deviation of 0.003 for large R and 0.005 for small R . As R tends to zero, the correlation energy approaches $-0.222\,222$, which is close to the exact value $-0.227\,411$. However, as R becomes large, one can show that $E^{\text{Hy}} \sim 1/(1.58R)$ which lies between the RHF and UHF energies. The Hylleraas wavefunction is thus a useful alternative to the small- and large- R solutions in the problematic intermediate region ($1 \lesssim R \lesssim 3$) with errors of 0.000, 0.0011 and 0.0021 for $R = 1, 2$ and 3 , respectively.

C. R12-CI

Using the Hylleraas wavefunction (67) as the reference for a CI expansion yields the R12-CI wavefunction

$$\Phi_L^{\text{R12-CI}}(\theta) = \hat{P} \Phi^{\text{Hy}}(\theta) + \sum_{\ell=1}^L T_\ell \Phi_\ell(\theta) \quad (72)$$

where

$$\hat{P} = \hat{I} - \sum_{\ell=1}^{\infty} |\Phi_\ell\rangle \langle \Phi_\ell| \quad (73)$$

is a projection operator that ensures orthogonality between the reference wavefunction and the excited determinants and \hat{I} is the identity operator. The coupling coefficients between two basis functions are the same as those for the conventional CI calculation (66) but with a correction for the matrix element

$$\begin{aligned} \langle \Phi^{\text{Hy}} | \hat{H} | \Phi_\ell \rangle &= \langle \Phi^{\text{RHF}} | \hat{H} | \Phi_\ell \rangle \\ &+ \gamma \frac{\ell(\ell+1)}{R\sqrt{2\ell+1}} \left(\frac{1}{2\ell+3} - \frac{1}{2\ell-1} \right) \end{aligned} \quad (74)$$

involving the ground state and the excited determinants. It is no longer possible to optimize γ in closed form so we used the value given by (70).

As Table III shows, the R12-CI energies converge much more rapidly with L than the CI energies and, for example, $E_2^{\text{R12-CI}}$ is more accurate than E_{40}^{CI} . This illustrates the importance of including a term that is linear in u . However, although this term enhances the *initial* convergence rate, the asymptotic behavior of the CI and R12-CI schemes are identical. Therefore, we now investigate the effect of including higher-order u terms.

D. Polynomial

In terms of the distance u , the Hamiltonian is

$$\hat{H} = \left(\frac{u^2}{4R^2} - 1 \right) \frac{d^2}{du^2} + \left(\frac{3u}{4R^2} - \frac{1}{u} \right) \frac{d}{du} + \frac{1}{u} \quad (75)$$

and a Kato-like analysis [25] reveals the cusp condition

$$\frac{\Phi'(0)}{\Phi(0)} = 1 \quad (76)$$

which deviates from the normal value of 1/2 [17].

The natural generalization of the Hylleraas wavefunction (67) is a polynomial and it is convenient to select the orthonormal basis of Jacobi polynomials [29]

$$\Xi_\ell(u) = \frac{\sqrt{\ell+1}}{4\pi R^2} P_\ell^{(1,0)} \left(1 - \frac{u}{R} \right) \quad (77)$$

and write the wavefunction as

$$\Phi_L^{\text{poly}} = \sum_{\ell=0}^L c_\ell \Xi_\ell(u) \quad (78)$$

The energy E_L^{poly} is the lowest eigenvalue of the matrix

$$\langle \Xi_i | \hat{H} | \Xi_j \rangle = \frac{(m^2 - 1)(\alpha m + \delta_{i,j})}{4R^2} + \frac{\alpha m}{R} \quad (79)$$

where $m = \min(i, j)$ and $\alpha = \sqrt{\frac{\min(i, j)}{\max(i, j)}}$.

Table III reveals the remarkable convergence of E_L^{poly} . Using $L = 40$ and $R = 1$, for example, we find

$$E_{40}^{\text{poly}} = 0.852\ 781\ 065\ 056\ 462\ 665\ 400\ 437\ 966\ 038\ 710 \\ 264\ 283\ 589\ 518\ 406\ 360\ 162\ 484\ 313\ 983 \quad (80)$$

The convergence is slower for larger values of R , but still impressive. For example, using $L = 40$ and $R = 1000$, the energy is still correct to 49 digits. The ease with which we can obtain these Schrödinger eigenvalues can be traced to the fact that the polynomial basis efficiently models all of the singularities (the 1st-order cusp, the third-order cusp, etc.) in the exact wavefunction.

In recent work [17], Seidl reported correlation energies based on his numerical integration of the Schrödinger equation from $\theta = 0$ to π using (4) and we have included these in Table II. It appears that some of his energies for small R are slightly inaccurate.

VII. CONCLUSION

In this article, we have reported results for the ground state of a simple two-electron system that is described by a single parameter R . Although we cannot solve its Schrödinger equation in closed form, we have found accurate wavefunctions and energies for small R (the weakly correlated limit) and large R (the strongly correlated limit). For $R \ll 1$, Møller-Plesset perturbation theory yields results close to the exact solution; for $R \gg 1$, accurate results can be found by considering the zero-point oscillations of the appropriate Wigner molecule.

We have also explored variational schemes that yield satisfactory results for all R . In particular, we have discovered a polynomial wavefunction that easily yields results of any required accuracy.

We believe that our results will be useful in the future development of accurate correlation functionals within density-functional theory [42, 43] and intracule functional theory [44–49].

Acknowledgments

PMWG thanks the APAC Merit Allocation Scheme for a grant of supercomputer time and Australian Research Council (Grant DP0664466) for funding. We also thank Yves Bernard for helpful comments on the manuscript, and fruitful discussions.

[1] P. Hohenberg and W. Kohn, Phys. Rev. B **136**, 864 (1964).

[2] W. Kohn and L. Sham, Phys. Rev. A **140**, 1133 (1965).

- [3] R. G. Parr and W. Yang, *Density Functional Theory for Atoms and Molecules* (Oxford University Press, 1989).
- [4] N. R. Kestner and O. Sinanoglu, Phys. Rev. **128**, 2687 (1962).
- [5] S. Kais, D. R. Herschbach, and R. D. Levine, J. Chem. Phys. **91**, 7791 (1989).
- [6] M. Taut, Phys. Rev. A **48**, 3561 (1993).
- [7] A. Alavi, J. Chem. Phys. **113**, 7735 (2000).
- [8] D. C. Thompson and A. Alavi, Phys. Rev. B **66**, 235118 (2002).
- [9] D. C. Thompson and A. Alavi, J. Chem. Phys. **122**, 124107 (2005).
- [10] D. C. Thompson and A. Alavi, Phys. Rev. B **69**, 201302 (2004).
- [11] E. Wigner, Phys. Rev. **46**, 1002 (1934).
- [12] G. S. Ezra and R. S. Berry, Phys. Rev. A **25**, 1513 (1982).
- [13] G. S. Ezra and R. S. Berry, Phys. Rev. A **28**, 1989 (1983).
- [14] P. C. Ojha and R. S. Berry, Phys. Rev. A **36**, 1575 (1987).
- [15] R. J. Hinde and R. S. Berry, Phys. Rev. A **42**, 2259 (1990).
- [16] J. W. Warner and R. S. Berry, Nature **313**, 160 (1985).
- [17] M. Seidl, Phys. Rev. A **75**, 062506 (2007).
- [18] M. Seidl, J. P. Perdew, and S. Kurth, Phys. Rev. Lett. **84**, 5070 (2000).
- [19] C. Møller and M. S. Plesset, Phys. Rev. **46**, 618 (1934).
- [20] E. A. Hylleraas, Adv. Quantum Chem. **1**, 1 (1964).
- [21] W. Kutzelnigg, Theor. Chim. Acta **68**, 445 (1985).
- [22] W. Klopper and W. Kutzelnigg, Chem. Phys. Lett. **134**, 17 (1987).
- [23] W. Klopper and W. Kutzelnigg, J. Phys. Chem. **94**, 5625 (1990).
- [24] W. Kutzelnigg and W. Klopper, J. Chem. Phys. **94**, 1985 (1991).
- [25] T. Kato, Commun. Pure Appl. Math. **10**, 151 (1957).
- [26] R. T. Pack and W. Byers Brown, J. Chem. Phys. **45**, 556 (1966).
- [27] A. Szabo and N. S. Ostlund, *Modern Quantum Chemistry : Introduction to Advanced Structure Theory* (Dover publications Inc., Mineola, New-York, 1989).
- [28] G. B. Arfken, *Mathematical Methods for Physicists* (Academic Press, New-York, 1966).
- [29] M. Abramowitz and I. A. Stegun, *Handbook of Mathematical Functions with Formulas, Graphs and Mathematical Tables* (Dover publications Inc., New-York, 1972).
- [30] J. Cizek and L. Paldus, J. Chem. Phys. **47**, 3976 (1967).
- [31] L. Paldus and J. Cizek, J. Chem. Phys. **52**, 2919 (1970).
- [32] R. Seeger and J. Pople, J. Chem. Phys. **66**, 3045 (1977).
- [33] A. R. Edmonds, *Angular Momentum in Quantum Mechanics* (Princeton University Press, 1957).
- [34] J. C. Slater, *Quantum Theory of Atomic Structures*, vol. 2 of *International Series in Pure and Applied Physics* (McGraw-Hill Book Compagny, Inc., 1960).
- [35] T. Helgaker, P. Jørgensen, and J. Olsen, *Molecular Electronic-Structure Theory* (John Wiley & Sons, Ltd., 2000).
- [36] P. M. W. Gill and D. P. O'Neill, J. Chem. Phys. **122**, 094110 (2005).
- [37] L. Lewin, *Dilogarithms and Associated Functions* (London: Macdonald, 1958).
- [38] M. Seidl, J. P. Perdew, and M. Levy, Phys. Rev. A **59**, 51 (1999).
- [39] M. Seidl, Phys. Rev. A **60**, 4387 (1999).
- [40] M. Seidl, Phys. Rev. A **75**, 042511 (2007).
- [41] C. M. Bender and T. T. Wu, Phys. Rev. **184**, 1231 (1969).
- [42] J. Sun, J. Chem. Theor. Comput. **5**, 708 (2009).
- [43] P. Gori-Giorgi, G. Vignale, and M. Seidl, J. Chem. Theor. Comput. **5**, 743 (2009).
- [44] P. M. W. Gill, D. L. Crittenden, D. P. O'Neill, and N. A. Besley, Phys. Chem. Chem. Phys. **8**, 15 (2005).
- [45] E. E. Dumont, D. L. Crittenden, and P. M. W. Gill, Phys. Chem. Chem. Phys. **9**, 5340 (2007).
- [46] D. L. Crittenden and P. M. W. Gill, J. Chem. Phys. **127**, 014101 (2007).
- [47] D. L. Crittenden, E. E. Dumont, and P. M. W. Gill, J. Chem. Phys. **127**, 141103 (2007).
- [48] Y. A. Bernard, D. L. Crittenden, and P. M. W. Gill, Phys. Chem. Chem. Phys. **10**, 3447 (2008).
- [49] J. K. Pearson, D. L. Crittenden, and P. M. W. Gill, J. Chem. Phys. **130**, 164110 (2009).